Theoretical study of the atomic structure of Pd nanoclusters deposited on a MgO(100) surface

W. Vervisch,[1] C. Mottet,[1] and J. Goniakowski[1,2]
[1]*CRMC2-CNRS, Campus de Luminy, Case 913, 13288 Marseille Cedex 9, France*
[2]*UFR Sciences de Luminy, Université de la Mediterranée, Marseille, France*
(Received 30 October 2001; revised manuscript received 1 March 2002; published 29 May 2002)

Using a mixed approach: a semiempirical potential for the metal bonding within the cluster, and a potential fitted to *ab initio* calculations for the metal-oxide interaction, we have studied Pd clusters deposited on the MgO(100) surface. Focusing our attention on the experimentally observed pyramidal form of the Pd deposits, we have analyzed the evolution of their morphology and atomic structure as a function of cluster size. In agreement with the experimental results, we find the ''flattened'' pyramids with truncated edges being energetically the most stable. We also observe a systematic tetragonal deformation of Pd at the interface, consisting of a lateral dilation of the lattice parameter (matching the lattice parameter of the substrate), accompanied by a reduction of the vertical separation between the Pd layers. As the size of Pd cluster increases, the lattice mismatch is no longer perfectly accommodated by the dilation of the Pd deposit, and a series of subsequent structural transitions within the deposit release partially its strain, driving to relatively well localized small zones where Pd atoms do not coincide with the preferential adsorption site of Pd on the MgO(100) surface. They can be seen as dislocation precursors giving a clear superstructure pattern at the interface.

DOI: 10.1103/PhysRevB.65.245411 PACS number(s): 68.35.−p, 68.47.Jn, 61.46.+w

I. INTRODUCTION

Whereas metallic, semiconducting, or oxide surfaces have given rise to a large amount of theoretical studies, there exist no standard and reliable methods for modeling the interfaces between materials of different character, in particular for metal-oxide ones. Indeed, most fundamental questions concerning the electronic structure, charge-density redistribution, or interface reactivity (interdiffusion of atoms across the interface) in these systems still remain unanswered,[1,2] and the character of interactions at the interface is still little known. Therefore, systematic theoretical studies based on approximations at a different level, and experimental investigations are necessary in order to better understand the basic microscopic mechanisms responsible for the cohesion at metal-oxide interfaces[1–5] (see Refs. 6 and 7 for a review).

Among these systems, Pd-MgO(100) is one of most largely used models of nonreactive metal-oxide interfaces, and it has given rise to many detailed experimental[6–22] and theoretical[23–34] studies. Although some of them have been motivated by the specific catalytic properties of the deposited metal,[7,35–37] on a more fundamental level, the analysis of substrate-induced modifications of the cluster morphology and atomic structure remains the principal tool towards a better understanding of interaction on the metal-oxide interface. Valid description of the latter seems possible within the *ab initio* methods that, contrary to most of existing semiempirical models,[23,25] reproduce the basic adsorption characteristics: the preferential adsorption site and the adsorption energy,[26,27] as reported in recent experimental studies.[18–20,22]

However, if first-principle calculations have been able to furnish data that agree well with some experimental results, the computational effort needed to model systems of a realistic size limits their field of application to model structures (pseudomorphy and periodic interfaces with very limited relaxation). It is still impossible to use them directly for studies on more complex interface geometries (inhomogeneous relaxations at the interface, reconstructions, dislocations, etc.) that have been observed experimentally. This fact complicates considerably any comparison between experimental and computational results (necessary to validate the employed approximations), limits seriously the practical interest of this kind of approaches, and shows the necessity to develop effective energetic models, able to treat more complex systems (larger sizes, lower symmetry, and systematic relaxation procedure), and better suited to reproduce the experimental complexity.

From this point of view the Pd/MgO(100) system seems particularly promising. On one hand, the Pd-MgO(100) interaction is relatively strong [contrary to what can be found, e.g., for Ag-MgO(100) (Refs. 38,39)], so that the energetic model is expected to be less sensitive to the approximations employed. On the other hand, the electron transfer at the Pd-MgO(100) interface is relatively small [contrary to what can be found, e.g., for metal-MgO(111) (Refs. 40–42)], so that cohesion of the metal deposit is expected to be only little modified by the substrate. Finally, in the case of the Pd-MgO(100), the existing experimental evidence is particularly rich: the grazing incidence x-ray scattering results by Renaud and Barbier[6,18–20] and the high resolution transmission electron microscopy (HRTEM) results by Graoui *et al.*[16,17] and Lu and Cosandey[43] give a relatively complete set of structural and energetic data, which can be used to validate the model. According to this experimental evidence, Pd particles prepared by UHV condensation and annealing are in cube-on-cube epitaxy on MgO(100) and present an octahedral shape limited by eight (111) faces and truncated by (001) facets on top and at the corners. The lattice parameters of the smallest Pd particles are dilated and accommodated to the MgO substrate. In larger ones this dilation is limited to at least three atomic layers at the interface. As the particle size increases, the strain is released by the introduction of misfit dislocations, which further organize into an ordered network, similar to what is found for bulk Pd-MgO interface.

The goal of our paper is twofold. On one hand, we propose a simple energetic model to describe the Pd-MgO(100) interface and confront its results with the existing experimental data. This comparison is used to check the validity of the model, to detect its deficiencies, and contributes directly to the general understanding of the microscopic mechanisms responsible for the cohesion on the metal-oxide interface. On the other hand, we propose a systematic and detailed study of the evolution of both the equilibrium morphology and the equilibrium atomic structure of deposited Pd clusters as a function of their size. Going beyond the accuracy of existing experimental characterization, they give a wide basis for discussion and interpretation of the experimental data and suggest keys to relate the specific reactivity properties of deposited Pd clusters to their size and morphology. They also furnish the basis necessary for any future study of Pd growth properties.

The paper is organized as follows. In Sec. II, we describe the energetic model (metal-metal and metal-oxide interactions) and the geometry optimization method (quenched molecular dynamics). The results concerning evolution of cluster morphology and of the atomic structure at the interface as a function of the cluster size are detailed in Sec. III. In the same section we present the results on calculated adhesion energies. Sec. IV is devoted to a discussion of the results and to conclusions.

II. ENERGETIC MODEL

A study of the atomic structure and morphology of supported metallic nanoclusters requires the determination of atomic configurations that minimize the total energy of the system. The existing minimum-search techniques, based on either quenched molecular dynamics or Monte Carlo approach, remain computationally very time consuming, and up to now they cannot be coupled with *ab initio* techniques of total energy calculations. For this reason, the present study relies on a semiempirical energetic model, in which we supply the relatively well established second moment approximation (SMA) potential derived from the electronic structure of the metal-metal interactions in the framework of the tight-binding model, with an analytical form of metal-MgO potential, which is obtained by fitting a set of model *ab initio* calculations.

A. Metal-metal interaction: Second moment approximation (SMA)

The SMA many-body potential has been widely used for metallic surface and cluster studies.[44–49] Within this model,[50] the band energy of each metal atom is proportional to the square root of the second moment of the local density of states, leading to the many-body character of the potential. The total energy of a cluster of N atoms is written as a sum of two terms: the band energy term (attractive part), and the repulsive term of the Born-Mayer type,

$$E^{Pd\text{-}Pd} = \sum_{i}^{N} \left\{ -\sqrt{\xi^2 \sum_{j} e^{-2q(r_{ij}/r_o-1)}} + A \sum_{j} e^{-p(r_{ij}/r_o-1)} \right\}, \tag{1}$$

where ξ is an effective hopping integral, r_{ij} is the distance between the atoms at sites i and j, r_o is the first-neighbor distance in the metal. The summation goes over all the neighbors up to the cutoff distance r_c. The parameters (ξ, A, q, p) are fitted to different experimental values: bulk cohesive energy (ϵ_B), lattice parameter (a),[51] and elastic constants $(B,\ C_{44},\ C')$ (Ref.52) of the metal. For Pd the parameters are $\xi = 1.702$ eV, $A = 0.171$ eV, $q = 3.794$, and $p = 11.0$. It is well known, not only in the SMA framework,[50] but also within similar methods such as the embedded-atom method,[53] or the corrected effective medium theory,[54] that fitting the value of the cohesive energy leads to underestimated values of the surface energy. In fact, within the present parametrization the energy of the Pd (100) surface σ_{100} is equal to 0.8 J/m^2, which is about one half of the experimental value (1.64 J/m^2).[55] Although not as precise as the *ab initio* methods,[56,57] the SMA approach describes correctly the relaxation and/or reconstruction of the low index surfaces.[44] Additionally, although the surface energies differ from the experimental estimations, the SMA approach gives a good anisotropy factor between the most compact surfaces. This latter, more than the absolute value of surface energy, is essential for the present study. In our case $\sigma_{100}/\sigma_{111} = 1.16$, which can be compared to *ab initio* results: 1.14 (Ref. 56) and 1.01 (Ref. 57) and to experimental estimation: 1.16.[16,17]

More generally, it has also to be kept in mind, that since the fitting procedure concerns principally the bulk characteristics, the representation of low-coordinated metal atoms (surfaces, clusters corners or edges) within the SMA potential is less good. In these cases, comparison of calculated and experimental results, e.g., for a Pd dimer, shows a tendency to overestimate the bond energy and underestimate the bond length.

B. Pd-MgO(100) interaction: Fit to *ab initio* results

The *ab initio* calculations used for the parametrization of the Pd-MgO potential were performed within the density-functional theory based on full-potential linearized augmented-plane wave (FPLAPW) method.[58] They are based on the hypothesis that the palladium-induced deformation of the substrate can be neglected.[59] In order to improve the description of the interaction energetics, we have used a gradient-corrected form of the exchange-correlation potential.[60] Further details on the computational settings used in the *ab initio* calculations are given in Ref. 34.

We have chosen to describe the interaction of the Pd cluster with the MgO substrate $E_{Pd\text{-}MgO}$ as a sum of contributions coming from all Pd atoms in the cluster. For each Pd atom i, its interaction with the substrate depends on its horizontal position (x,y) with respect to the MgO lattice, and on its elevation z above the MgO surface. In order to take into account the many-body effects responsible for the weakening of interactions as a function of an increasing number of

neighbors, for each considered Pd atom we have included explicitly the dependence of the Pd-MgO interaction on the number of its nearest Pd neighbors Z,

$$E^{Pd\text{-}MgO}=\sum_{i=1}^{N} E_i(x,y,z,Z), \tag{2}$$

where N is the number of Pd atoms in the cluster.

We have used a simple analytical formula to describe the dependence of the $E_i(x,y,z,Z)$ term on the elevation z of the Pd atom,

$$E_i(x,y,z,Z)=a_1+e^{-2a_2(z-a_3)}-2e^{-a_2(z-a_3)}. \tag{3}$$

As explained below, parameters a_i contain the information on dependence of the interaction energy on (x,y) and Z.

Results of *ab initio* calculations show clearly that the interaction of Pd adatoms with MgO substrate depends on the Pd coverage.[29] As expected, it is the strongest in the case of adsorption of isolated adatoms and decreases progressively as a function of the growing number of Pd-Pd neighbors. In order to take into account this dependence in the interaction potential we have performed *ab initio* calculations for three model Pd deposits: isolated Pd atoms, epitaxial Pd monolayer, and epitaxial Pd bilayer, which correspond to Pd nearest-neighbor numbers of 0, 4, and 8, respectively, and thus cover in an uniform manner the coordination numbers going from isolated adatoms up to the fully constituted Pd-MgO(100) interface.[34] A three-point interpolation formula describing the dependence of the interaction energy on the coordination of the Pd atom Z used in the parametrization reads

$$a_i(x,y,Z)=b_{i1}+b_{i2}e^{-Z/b_{i3}}, \tag{4}$$

where parameters b_{ij} are further dependent on (x,y).

The MgO(100) surface has a square lattice with two atoms per unit cell. Due to its symmetry, the periodic surface unit cell can be constructed from eight irreducible triangles, each of them expanded over a surface oxygen, a surface magnesium, and a surface hollow site. The *ab initio* calculations show that regardless of the metal coverage the oxygen site is the most energetically favorable for adsorption of Pd (minimum in the potential energy surface), the magnesium site is the less energetically favorable (maximum in the potential energy surface), the hollow site being intermediate (saddle point in the potential energy surface).[27] By preserving the model epitaxial geometry of the deposits in the periodic *ab initio* calculations, we were able to relate the calculated adsorption energetics to particular surface adsorption sites. A three-parameter interpolation from these three high-symmetry points to all intermediate (x,y) positions of the Pd atom is taken as a linear combination of trigonometric functions preserving the symmetry of the surface unit cell,

$$b_{ij}(x,y)=c_{ij1}+c_{ij2}[\cos(x)+\cos(y)]+c_{ij3}[\cos(x+y)+\cos(x-y)]. \tag{5}$$

In this way, we obtain a 27 parameters analytical formula which interpolates between about 100 points issued from *ab initio* calculations. Figure 1 resumes the calculated points and the fitted dependences.

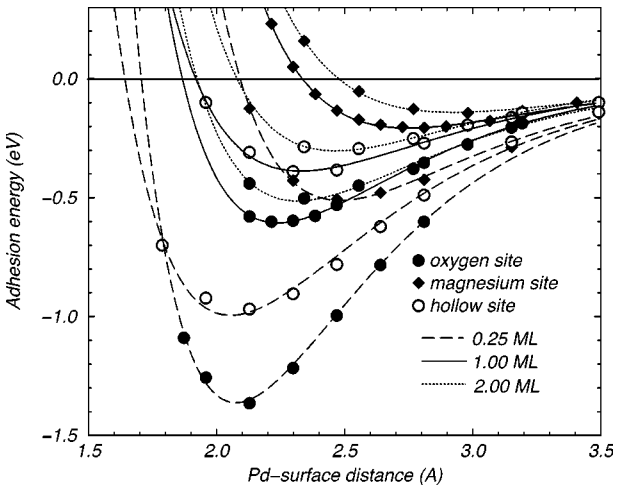

FIG. 1. Dependence of the adsorption energy of Pd on the MgO(100) surface on the Pd coverage, and on the position of adsorbed Pd atoms. Circles represent the results of *ab initio* FPLAPW calculations, the lines represent the fitted analytical expression for the Pd-MgO interaction.

A comment on the parametrization of the Pd-MgO(100) interaction seems necessary. The adsorption energies extracted from the *ab initio* calculations correspond to the total energy difference between the constituted system [Pd-MgO(100)] and the two separated components [floating Pd deposit and clean MgO(100) surface]. This procedure has the advantage to include not only the energy of the direct Pd-MgO interaction, but also the contribution due to the adsorption-induced changes of cohesion in both substrate and adsorbate. Since in our present parametrization the Pd-Pd potential is not modified as to account for the adsorption-induced decohesion in the Pd deposit,[31] we may thus underestimate the expected dilation of the Pd interatomic distances.

III. RESULTS

We use quenched molecular dynamics (QMD) algorithm[61] to relax the atomic structure of the cluster towards its energy minimum. The quenching procedure in which the velocity of the atoms is canceled when it opposes the force acting on the atom leads to the minimization of the potential energy of the system at 0 K.[62]

As explained above, the MgO substrate is kept rigid during the minimization.

A. Evolution of cluster morphology as a function of cluster size

All the UHV results on Pd deposition on the MgO(100) surface agree on a three-dimensional growth (Volmer-Weber) involving nucleation, growth and coalescence of clusters following the cube-cube pseudomorphy.[6–21]. For that reason, we have focused our attention on deposition of truncated Pd octahedra,[17] oriented as to satisfy the [100]Pd//[100]MgO

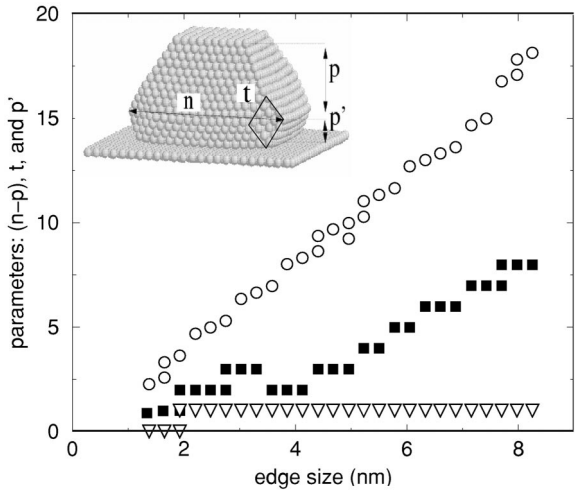

FIG. 2. Inset, n, p, t, and p' parameters used for cluster morphology characterization. The truncations $(n-p)$ (empty circles) and t (squares) and the number or reentering layers p' (empty triangles) are given as a function of the edge size n.

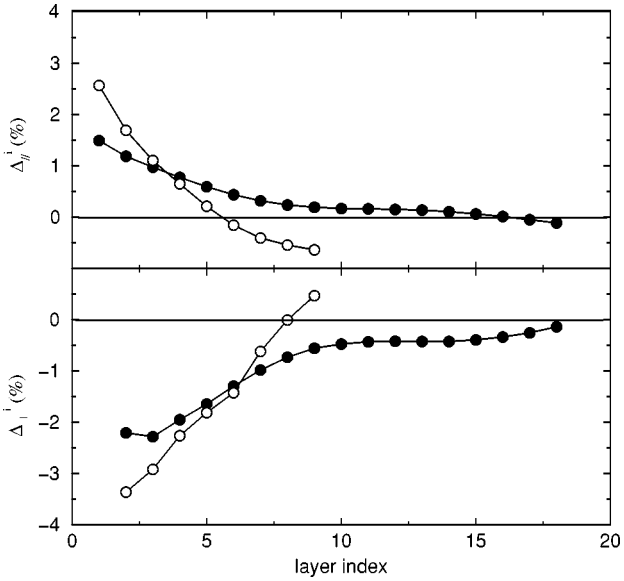

FIG. 3. Substrate-induced modifications of structural parameters: $\Delta_{\parallel}^{i}=(\langle d_{\parallel}\rangle_{sup.}^{i}-\langle d_{\parallel}\rangle_{free}^{i})/\langle d_{\parallel}\rangle_{free}^{i}$ and $\Delta_{\perp}^{i}=(\langle d_{\perp}\rangle_{sup.}^{i}-\langle d_{\perp}\rangle_{free}^{i})/\langle d_{\perp}\rangle_{free}^{i}$ as a function of the layer index i. Filled circles correspond to the (12,8,1,3) cluster and empty circles to the (26,17,1,7) cluster. $i=1$ corresponds to the interfacial Pd layer and $i=9$ or $i=18$ to the (100) upper facets of the two clusters, respectively.

epitaxy relation. In fact, for clusters sizes considered in the present study, we have never stabilized any disoriented structure, and always recovered the perfect cube-cube pseudomorphy.

In order to analyze the modifications of the morphology as a function of cluster size, we have considered various clusters, as defined by the set of four parameters illustrated in the inset of Fig. 2. Namely, for each size of the cluster edge n, we have considered several different cluster heights p, corner truncations t, and number of reentering atomic layers p'.

For the sake of a synthetic analysis of the evolution of cluster morphology and atomic structure as a function of their size, we have chosen two different series of clusters corresponding to two particular morphologies. The first one is simply a series of perfect pyramids, with no truncation $(p=n,t=p'=0)$. The second one is the series in which, for each n we have chosen the form that minimizes the cluster energy. In the following we will refer to this series as the ''minimum energy'' one. The corresponding values of the n, p, t, and p' parameters are represented in Fig. 2. Both these choices may seem somewhat arbitrary, but since the two series represent clusters with drastically different stabilities, it is interesting to see if the calculated deposit properties depend on the detailed morphology and to what extent the conclusions of the present study are general.

Looking at Fig. 2 we can distinguish two regimes in the evolution of the truncations $(n-p)$ and t as a function of n: at small sizes (less than 4 nm), the most favorable structure corresponds to a half truncated pyramid [$(n-p)$ increases linearly with n with a slope of 1/2 corresponding to the aspect ratio], and only the lateral corner atoms are missing (t is constant and equal to 1 or 2). Such a morphology has effectively been observed experimentally for the smallest sizes (1–3 nm).[17] As the size increases, the lateral truncation t increases in parallel to $(n-p)$. Such an evolution is typically in accordance with the Wulff theorem and is in good agreement with the experimental results for sizes larger than 4 nm.[17] Finally, starting from a relatively small size, a single reentrant layer appears to stabilize energetically the deposited clusters. Contrary to what could be expected, we do not observe any evolution of p' as a function of the cluster size. This can be explained by an effect of local coordination number. Indeed, the introduction of the reentrant layer increases the coordinations of the atoms at the cluster edges from $Z=5$ to $Z=7$. As observed experimentally,[17] for larger sizes, one could expect an extension of the reentrant facets.

B. Evolution of the clusters atomic structure as a function of cluster size

In order to better characterize the structure of the deposited clusters and to analyze efficiently their dependence on the cluster size we have used two parameters: the average nearest neighbor distance between the Pd atoms within the ith atomic layer parallel to the substrate ($i=1$ for the interfacial Pd layer): $\langle d_{\parallel}\rangle^{i}$, and the average nearest neighbor distance between atoms in two subsequent Pd atomic layers: $\langle d_{\perp}\rangle^{i}$. Figure 3 shows the substrate-induced modifications of these two parameters with respect to the corresponding free (unsupported) clusters in the case of $(n,p,p',t)=(12,8,1,3)$ and (26,17,1,7).

Two main points have to be noticed. On one hand, the deposition-induced effects correspond to what can be called a tetragonal deformation, and consist in an horizontal dilation of the average Pd-Pd distances ($\sim 2\%$) accompanied by a contraction of the vertical interlayer spacing ($\sim 3\%$). The dilation of the horizontal interatomic distances compensates partially the lattice mismatch between the two materials

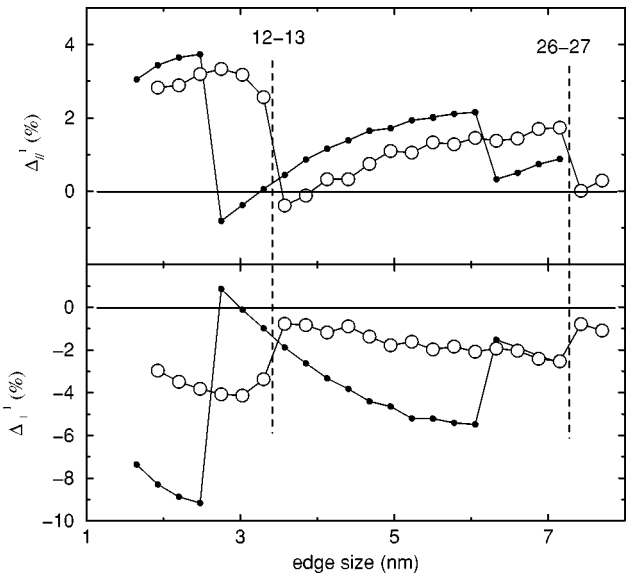

FIG. 4. Evolution of the structural parameters $\Delta_{\parallel}^{1}$ and $\Delta_{\perp}^{1}$ as a function of the cluster size, as given by the cluster edge length (nm). Results for both perfect pyramids (full circles) and ''minimum-energy'' structures (empty circles) are shown.

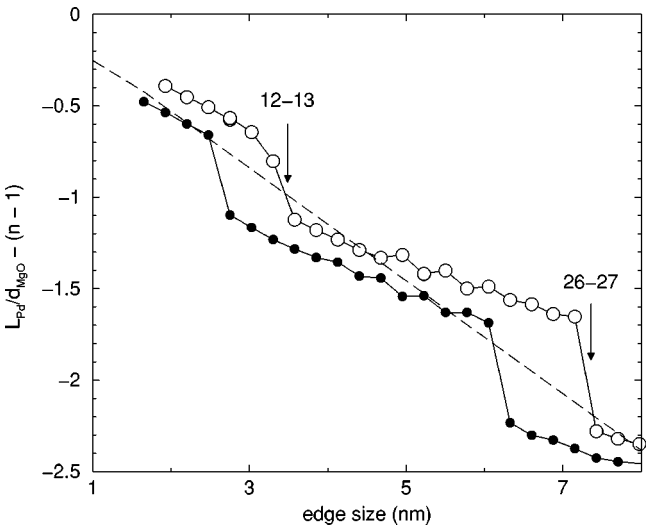

FIG. 5. Calculated evolution of the epitaxy parameter between the Pd and MgO lattices as a function of the edge length L_{Pd} for the ''minimum-energy'' structures (empty circles), for the perfect pyramids (full circles), and for an incommensurate interface (dashed line).

(8%). The tetragonal character of the deformation results from the well-known tendency of metals to conserve their atomic volume upon a deformation. On the other hand, this substrate-induced deformation is the strongest for atomic layers in direct contact with the substrate and decreases rapidly as the layer index *i* increases. Whereas the small cluster is deformed in its whole volume, the big cluster recovers the bulk lattice parameter in its core. As a consequence, the upper facet of the small cluster is still significantly perturbed by the substrate.

Such an expansion of the palladium lattice parameter has been observed *ex situ* by HRTEM[9] or by grazing incidence x-ray scattering[19] and confirmed *in situ* by surface electron energy-loss fine-structure spectroscopy.[12] The authors[17] show additionally that for small sizes (less than 2–3 nm) the whole cluster is strained whereas for bigger sizes (4–6 nm) the deformation is localized near the interface in the first three layers.

In Fig. 4 we present the calculated evolution of the deformation parameters $\Delta_{\parallel}^{1}$ and $\Delta_{\perp}^{1}$ as a function of cluster size, as obtained for both the ''minimum energy'' series and for the perfect pyramids. The variation of the $\Delta_{\parallel}^{1}$ and $\Delta_{\perp}^{1}$ is characterized by regions in which the tetragonal deformation increases slowly as a function of cluster size, separated by its abrupt reduction, which we will associate with transitions between different atomic structures of the Pd-MgO(100) interface. Very clearly, these transitions occur at different sizes for clusters of different morphology: for the edge lengths *n* of 9–10 (i.e., around 2.6 nm) and 22–23 (6.2 nm) for the perfect pyramids, and for the edge lengths *n* of 12–13 (3.4 nm) and 26–27 (7.3 nm) for the ''minimum energy'' series. It is, however, to be noticed that in the size range studied here, regardless of the considered cluster morphology, the two transitions are separated by about 3 nm, which can be seen as a signature of a periodic superstructure at the interface.

It is interesting to relate the modifications of the atomic structure of the clusters to that of the Pd-MgO(100) interface. In order to do this we have calculated the epitaxy parameter $L_{Pd}/d_{MgO}-(n-1)$ (where L_{Pd} is the edge length of the Pd cluster and $d_{MgO}=a_{MgO}/\sqrt{2}=3.01$ Å is the distance between two oxygen adsorption sites on the rigid MgO substrate). This parameter quantifies the matching of the two lattices: it is equal to zero for a coherent epitaxy (pseudomorphy), and it varies linearly as a function of cluster size for an incommensurate interface. The results obtained for the two considered series are given in Fig. 5. The two series display a similar behavior: regions of constant slope (intermediate between pseudomorphic and incommensurate structures), separated by abrupt drops, which can be associated with the structural transitions mentioned above (see Fig. 4). The former correspond to the progressive dilation of Pd-Pd interatomic distances, whereas the latter indicate Pd stress release, the dilation of Pd lattice vanishing.

C. Local structure at the interface: Characterization of the structural transitions

The above analysis is based on average structural parameters, and does not account for local modifications at the interface, which are responsible in the strongly nonmonotonic evolution of the tetragonal deformation as a function of the cluster size.

In order to elucidate the mechanism responsible for the transitions we have calculated the local atomic pressure at each of the Pd atomic sites in the interfacial layer. Such quantity can be defined as[63]

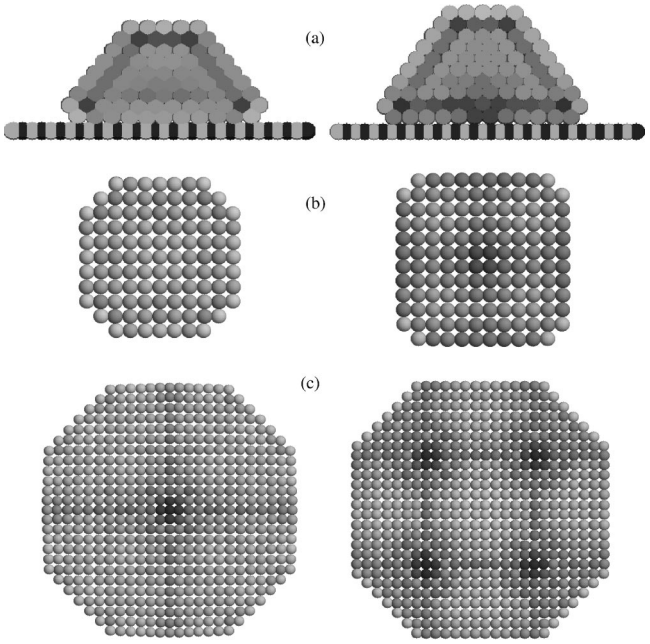

FIG. 6. Pressure maps on the atomic sites across the Pd cluster along a cutting plane perpendicular to the substrate (a), on the interfacial Pd layer (b) and (c). The left-hand column corresponds to clusters $n=12$ (a, b) and $n=26$ (c), the right-hand column corresponds to clusters $n=13$ (a, b) and $n=27$ (c). Dark zones correspond to high positive pressure (compression) whereas bright zones correspond to no or to negative pressure (tension).

$$P_i^{Pd} = -\frac{d(E^{Pd\text{-}Pd} + E^{Pd\text{-}MgO})}{d \ln V_i}, \tag{6}$$

where V_i is the atomic volume at site i. A positive/negative sign indicates a compressive/tensile strain. Although this quantity is not directly comparable with experimental measurements, it has proven[64] to be a useful tool for a qualitative analysis of the nature and localization of strain states and for prediction of structural modifications (e.g., misfit dislocations) in order to release the strain.

The pressure maps [Fig. 6(a), along a cutting plane perpendicular to the substrate] display three interesting effects. First, the deformation induced by the substrate concerns essentially a few Pd planes in the neighborhood of the interface, then the cluster core recovers a bulklike pressure, i.e., a near zero pressure. Second, the surface of the cluster is globally in tension, although the interatomic distances are contracted, because the surface sites are less coordinated. In fact, perpendicular to the cluster surface, one recovers an oscillating profile with contraction/dilation of interatomic distances in the same way as the infinite surfaces.[44] Finally, for $n=12$, the interface is nearly pseudomorphic (11 Pd rows per 11 surface oxygen rows), whereas for $n=13$ the pseudomorphy vanishes (12 Pd rows per 11 surface oxygen rows) resulting in an incommensurate interface (cf. Fig. 5). As a consequence, the interface Pd layer is in tension in the $n=12$ cluster (related to the substrate-induced expansion of Pd-Pd distances) and exhibits a small zone of compression in the center in the $n=13$ cluster (related to the fact that Pd atoms are on top of surface Mg atoms) [cf. Fig. 6(b) right-hand column]. This zone corresponds to the crossing of two additional $\langle 110 \rangle$ and $\langle 1\bar{1}0 \rangle$ Pd rows, which could be considered as dislocation precursors, and can be clearly distinguished at bigger cluster size ($n=26$) [cf. Fig. 6(c), left-hand column]. At $n=27$, the second structural transition introduces new compression zones [cf. Fig. 6(c), right-hand column], related to a network of such precursors, which can be associated with the Burgers vector of type $b=a_{Pd}/2\langle 110 \rangle$. This is in agreement with experimental results obtained for large clusters[17,19] and for infinite interface.[43]

We have limited our study to the appearance of the second transition but it can be expected that the system will display subsequent transitions leading to a (10×10) superstructure at the interface. The corresponding lattice parameter is somewhat smaller than the spacing between the dislocation lines given by $a_{MgO}/(a_{MgO}-a_{Pd})|b|$,[43] what can be associated with the finite cluster size.

Very clearly, the interface structure cannot be reduced to a simple pseudomorphy or to an incommensurate structure but presents a superstructure related to the size mismatch between the two materials.

D. Adhesion energy of the interface: Origin of the structural transitions

In order to identify the physical origin of the observed transitions of the atomic structure at the interface, we have analyzed in some details the evolution of the Pd-MgO(100) adhesion energy as a function of the cluster size. In our case, the Pd-MgO contact area being finite, we define the adhesion energy of the Pd cluster on the MgO substrate as

$$E_{adh} = \frac{1}{N_{int}}(E_{sup}^{Pd\text{-}MgO} - E_{free}^{Pd} - E_{clean}^{MgO}), \tag{7}$$

where $E_{sup}^{Pd\text{-}MgO}$ is the optimized energy of a Pd cluster deposited on the MgO surface, E_{free}^{Pd} and E_{clean}^{MgO} are, respectively, the energies of the free cluster (of the same morphology as the one deposited but with relaxed atomic distances) and of the MgO substrate. N_{int} is the number of Pd atoms in the interfacial layer. Since $E_{sup}^{Pd\text{-}MgO}$ is a sum of contributions due to Pd-Pd interactions $E_{sup}^{Pd\text{-}Pd}$ and to metal-substrate interaction $E^{Pd\text{-}MgO}$ and $E_{free}^{Pd} = E_{free}^{Pd\text{-}Pd}$, the above expression can be rewritten in order to separate these two terms,

$$E_{adh} = \frac{1}{N_{int}}(E_{sup}^{Pd\text{-}Pd} - E_{free}^{Pd\text{-}Pd}) + \frac{1}{N_{int}}(E_{sup}^{Pd\text{-}MgO} - E_{clean}^{MgO}). \tag{8}$$

The first term of this equation called $E_{adh}^{Pd\text{-}Pd}$ represents the energy loss related to the substrate-induced structural deformation of the Pd cluster, the second term called $E_{adh}^{Pd\text{-}MgO}$ is the energy gain related to the interaction with the MgO(100) surface. The evolution of the total adhesion energy and of its two components as a function of the cluster size is depicted in Fig. 7 for the perfect pyramids and for the ''minimum-energy'' series.

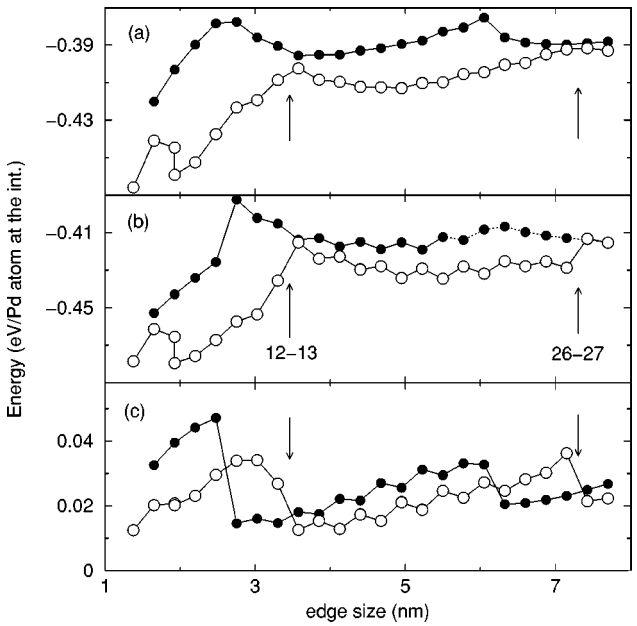

FIG. 7. Adhesion energy E_{adh} (a) for the perfect pyramids (full circles) and the ''minimum-energy'' series (empty circles) decomposed into: $E_{adh}^{Pd\text{-}MgO}$ (b) and $E_{adh}^{Pd\text{-}Pd}$ (c) as a function of cluster size. The two structural transitions between clusters $n=12$ and $n=13$, and between $n=26$ and $n=27$, are marked with arrows.

As expected, the $E_{adh}^{Pd\text{-}Pd}$ component is always positive, which in the present sign convention, corresponds to a term that acts against the adhesion. It can be related to the energy loss due to the deposition-induced deformation of the atomic structure of the clusters. Additionally, its evolution along the series follows directly the deformation strength, as illustrated in either Fig. 4 or Fig. 5. Both structural transitions tend to reduce the average deformation of the cluster and reduce the related Pd-Pd energy expense. Not surprisingly, the $E_{adh}^{Pd\text{-}MgO}$ is in all cases negative and represents the stabilizing effect. Its evolution along the series reflects the changes in the occupation of the preferential adsorption sites by the Pd atoms in the interfacial layer. For all cluster sizes it is the $E_{adh}^{Pd\text{-}MgO}$ contribution that dominates the overall deposition energetics, the contribution related to the relaxation of the Pd deposit being by one order of magnitude smaller.

When looking at the ''minimum-energy'' series at small sizes, we can notice a first drop of the E_{adh} around 2 nm edge size. This is induced by the reentrant atomic layer coming out, which by eliminating the most undercoordinated atoms in the cluster, improves significantly the epitaxial relation.

Variations of E_{adh} as a function of cluster size become weaker for larger cluster sizes and we observe a convergence towards the value of 0.39 eV/Pd atom (0.83 J/m^2), which is in good agreement with the experimental estimation by Graoui *et al.*[17] (0.75–0.91 J/m^2) obtained for large particles (10–15 nm). One could expect that at larger sizes, when edge effects are no longer predominant, the cluster morphology verifies the Wulff-Kaishev theorem.[17,65] In fact, our aspect ratio $p/n\sim 0.5$ is consistent with the fact that $W\sim\sigma_{100}$ in our model. Due to the underestimation of σ_{100} in our model as mentioned in Sec. II A, our aspect ratio is somewhat smaller than the experimental estimation (0.7).[17]

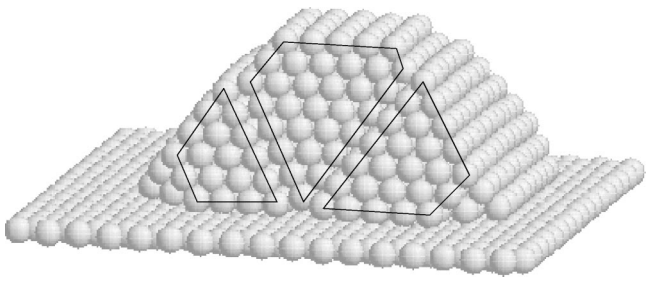

FIG. 8. Schematic representation of the dislocated cluster structure.

E. Alternative structure: dislocated Pd clusters

In a relatively narrow range of cluster sizes, an extensive search of energy minima has produced an another type of interesting atomic structure on which we would like to focus in the following. This structure, represented schematically in Fig. 8, shows clearly a local mismatch adjustment at the interface. The first Pd plane separates in its middle into two less dilated domains, leading to an almost missing Pd $\langle 110\rangle$ row. In order to fill this empty space, Pd atoms move along the two sliding (111) planes forming a prismatic structure.

This new atomic structure becomes energetically the most favorable around the first structural transition, where nondislocated clusters suffer the weakest stability (around $n=12$–13). As the size of cluster and their adhesion increase, it quickly becomes metastable.

Although for the small sizes the brief appearance of this alternative structure may be considered as somewhat anecdotical, it reveals the existence of an alternative way to accommodate the interface misfit. Although, not easy to be found by the QMD runs, for larger cluster sizes it could be seen as an extension of the dislocation precursor that has been discussed in the preceding section.

IV. CONCLUSIONS

Using a semiempirical potential for the metal bonding within the cluster, and a potential fitted to *ab initio* calculations for the metal-oxide interaction, we have studied the equilibrium atomic structure of small Pd clusters deposited on the MgO(100) surface as a function of their size.

In agreement with the experimental results we find the ''flattened'' pyramids with truncated edges energetically the most stable and observe systematically a tetragonal deformation of Pd at the interface. It consists of a lateral dilation of Pd lattice parameters (to match the lattice of the substrate), accompanied by a contraction of the vertical separation between the Pd layers (to keep constant the volume/atom in the metal). For small particles this deformation is relatively strong and propagates within all the cluster. For bigger sizes, while a precursor of a misfit dislocation appears at the interface, the tetragonal deformation becomes weaker and more localized to the interfacial region. As the size of clusters increases, a series of subsequent structural transitions release

partially the strain, introducing a network of [110] dislocation precursors. The resulting (10×10) superstructure at the interface is characteristic of the bulk Pd-MgO(100) interface. Adhesion energy decreases as the cluster size increases, following closely the occupation of the preferential adsorption sites. The strain-induced energy of Pd deposit is in all cases small.

Our study brings also details of atomic structure that go beyond the current experimental evidence. This concerns the appearance of first interface misfit dislocation precursor, or the presence of a single reentrant atomic layer already for relatively small clusters. This second effect can be one factor determining the peculiar reactivity of Pd atoms at the cluster edges. By taking fully into account the relaxation within deposited clusters, our investigations go beyond the existing theoretical studies on model pseudomorphic metal-oxide interfaces. This allows us to propose mechanisms of strain release at the interface, and to give a new insight into the coupling between the nature of interaction and the atomic structure of the interface.

ACKNOWLEDGMENTS

We thank C. Noguera, S. Giorgio, G. Tréglia, B. Legrand, and C. Henry for their interest and stimulating discussions. The most time consuming calculations were performed on the NEC-SX5 computer at IDRIS, under Project No. 960732. We are grateful for a generous allocation of time on the machine.

[1] V.E. Henrich and P.A. Cox, *The Surface Science of Metal Oxides* (Cambridge University Press, Cambridge, 1994).
[2] C. Noguera, *Physics and Chemistry at Oxide Surfaces* (Cambrige University Press, Cambridge, 1995).
[3] M.W. Finnis, J. Phys.: Condens. Matter **8**, 5811 (1996).
[4] F. Didier and J. Jupille, Surf. Sci. **314**, 378 (1994).
[5] H.J. Freund, H. Kuhlenbeck, and V. Staemmler, Rep. Prog. Phys. **59**, 283 (1996).
[6] G. Renaud, Surf. Sci. Rep. **32**, 1 (1998).
[7] C.R. Henry, Surf. Sci. Rep. **31**, 231 (1998).
[8] C. Goyhenex, Ph.D. thesis, Marseille, 1996.
[9] S. Giorgio, C.R. Henry, C. Chapon, and J.M. Penisson, J. Cryst. Growth **100**, 254 (1990).
[10] C.R. Henry, C. Chapon, C. Duriez, and S. Giorgio, Surf. Sci. **253**, 177 (1991).
[11] S. Giorgio, C. Chapon, C.R. Henry, and G. Nihoul, Philos. Mag. B **67**, 773 (1993).
[12] C. Goyhenex, C.R. Henry, and J. Urban, Philos. Mag. A **69**, 1073 (1994).
[13] M. Meunier and C.R. Henry, Surf. Sci. **307-309**, 514 (1994).
[14] H. Fornander, A.J. Birch, L. Hulman, L.G. Peterson, and J.E. Sundgren, Appl. Phys. Lett. **68**, 2636 (1996).
[15] H. Fornander, L. Hulman, A.J. Birch, and J.E. Sundgren, J. Cryst. Growth **186**, 189 (1998).
[16] H. Graoui, S. Giorgio, and C.R. Henry, Surf. Sci. **417**, 350 (1998).
[17] H. Graoui, S. Giorgio, and C.R. Henry, Philos. Mag. B **81**, 1649 (2001).
[18] G. Renaud and A. Barbier, Surf. Sci. **433-435**, 142 (1999).
[19] G. Renaud, A. Barbier, and O. Robach, Phys. Rev. B **60**, 5872 (1999).
[20] G. Renaud and A. Barbier, Appl. Surf. Sci. **142**, 14 (1999).
[21] H. Fornander, A.J. Birch, P. Sandstrom, and J.E. Sundgren, Thin Solid Films **349**, 4 (1996).
[22] G. Haas, A. Menck, H. Brune, J.V. Barth, J.A. Venables, and K. Kern, Phys. Rev. B **61**, 11 105 (2000).
[23] D.M. Duffy, J.H. Harding, and A.M. Stoneham, Philos. Mag. A **67**, 865 (1993).
[24] R-q. Wu and A.J. Freeman, Phys. Rev. B **51**, 5408 (1995).
[25] K. Yamamoto, Y. Kasukabe, R. Takeishi, and T. Osaka, J. Vac. Sci. Technol. A **14**, 327 (1996).
[26] I.V. Yudanov, G. Pacchioni, K.M. Neyman, and N. Rösch, J. Phys. Chem. B **101**, 2786 (1997).
[27] J. Goniakowski, Phys. Rev. B **57**, 1935 (1998).
[28] R. Yamauchi, M. Kubo, A. Miyamoto, R. Vetrivel, and E. Broclawik, J. Phys. Chem. B **102**, 795 (1998).
[29] J. Goniakowski, Phys. Rev. B **58**, 1189 (1998).
[30] A.M. Ferrari, C. Xiao, K.N. Neyman, G. Pacchioni, and N. Rösch, Phys. Chem. Chem. Phys. **1**, 4655 (1999).
[31] J. Goniakowski, Phys. Rev. B **59**, 11 047 (1999).
[32] A.V. Matveev, K.M. Neyman, I.V. Yudanov, and N. Rösch, Surf. Sci. **426**, 123 (1999).
[33] J. Oviedo, J. Fernández Sanz, N. López, and F. Illas, J. Phys. Chem. B **104**, 4342 (2000).
[34] L. Giordano, J. Goniakowski, and G. Pacchioni, Phys. Rev. B **64**, 075417 (2001).
[35] C.R. Henry, C. Chapon, C. Goyhenex, and R. Monot, Surf. Sci. **272**, 283 (1992).
[36] C. Goyhenex, M. Croci, C. Claeys, and C.R. Henry, Surf. Sci. **353**, 475 (1996).
[37] L. Piccolo and C.R. Henry, Appl. Surf. Sci. **163-163**, 670 (2000).
[38] Y. Yao and Y. Zhang, Phys. Lett. A **256**, 391 (1999).
[39] J.A. Purton, D.M. Bird, S.C. Parker, and D.W. Bullett, J. Chem. Phys. **110**, 8090 (1999).
[40] R. Benedek, D.N. Seidman, M. Minkoff, L.H. Yang, and A. Alavi, Phys. Rev. B **60**, 16 094 (1999).
[41] J. Goniakowski and C. Noguera, Phys. Rev. B **60**, 16 120 (1999); *ibid.* (to be published).
[42] R. Benedek, A. Alavi, D.N. Seidman, L.H. Yang, D.A. Muller, and C. Woodward, Phys. Rev. Lett. **84**, 3362 (2000).
[43] P. Lu and F. Cosandey, Acta Metall. Mater. **40**, S259 (1992).
[44] M. Guillopé and B. Legrand, Surf. Sci. **215**, 577 (1989).
[45] R. Ferrando and G. Tréglia, Phys. Rev. B **50**, 12 104 (1994).
[46] A. Khoutami, B. Legrand, C. Mottet, and G. Tréglia, Surf. Sci. **307**, 735 (1994).
[47] C. Mottet, G. Tréglia, and B. Legrand, Surf. Sci. Lett. **383**, L719 (1997).
[48] F. Montalenti and R. Ferrando, Phys. Rev. B **59**, 5881 (1999); Phys. Rev. Lett. **82**, 1498 (1999).

[49] F. Baletto, C. Mottet, and R. Ferrando, Surf. Sci. **446**, 31 (2000); Phys. Rev. Lett. **84**, 5544 (2000); F. Baletto, R. Ferrando, A. Fortunelli, F. Montalenti, and C. Mottet, J. Chem. Phys. **116**, 3856 (2002).

[50] V. Rosato, M. Guillopé, and B. Legrand, Philos. Mag. A **59**, 321 (1984).

[51] C. Kittel, *Introduction to Solid State Physics* 7th ed. (Wiley, New York, 1996).

[52] G. Simmons and H. Wang, *Single Crystal Elastic Constants and Calculated Aggregated Properties* (MIT, Cambridge, 1971).

[53] S.M. Foiles, M.I. Baskes, and M.D. Daw, Phys. Rev. B **33**, 7983 (1986).

[54] M.S. Stave, D.E. Sanders, T.J. Reaker, and A.E. DePristo, J. Chem. Phys. **93**, 4413 (1990).

[55] C.L. Liu, J.M. Cohen, J.B. Adams, and A.F. Voter, Surf. Sci. **253**, 334 (1991).

[56] M. Methfessel, D. Henning, and M. Scheffler, Phys. Rev. B **46**, 4816 (1992).

[57] H.L. Skriver, and N.M. Rosengaard, Phys. Rev. B **46**, 7157 (1992).

[58] P. Blaha, K. Schwarz, and J. Luitz, WIEN97 (Vienna University of Technology, Vienna, 1997); This is an improved and updated UNIX version of the original copyrighted WIEN code, which was published by P. Blaha, K. Schwarz, P. Sorantin, and S.B. Trickey, Comput. Phys. Commun. **59**, 399 (1990).

[59] *Ab initio* calculations performed on the bulk materials show that the energy necessary to deform tetragonally bulk Pd as to fit the lattice parameters of bulk MgO is about six times smaller than that required for the equivalent deformation of bulk MgO. Additionally, we have performed *ab initio* calculations of adsorption of a single Pd atom, with and without relaxation of the substrate. In this case, where the interaction between the substrate and the adsorbate is stronger than in the case of the extended interface, relaxation of MgO modifies the adsorption energy and the adsorption height by less than 2%. This confirms a relatively limited role of substrate relaxation on the adsorption characteristics. We will come back to this question in a forthcoming paper.

[60] J.P. Perdew, K. Burke, and Y. Wang, Phys. Rev. B **54**, 16 533 (1996).

[61] L. Verlet, Phys. Rev. **159**, 98 (1967).

[62] C.H. Bennett, in *Diffusion in Solids, Recent Developments*, edited by A.S. Nowick and J.J. Burton (Academic, New York, 1975), p. 73.

[63] P.C. Kelires and J. Tersoff, Phys. Rev. Lett. **63**, 1164 (1989).

[64] G. Tréglia, in *Stress and Strain in Epitaxy: Theoretical Concepts, Measurements and Applications*, edited by M. Hanbücken and J.P. Deville (Elsevier, Amsterdam, 2001), p. 119.

[65] R. Kaishew, Bull. Acad. Sci. Ser. Phys. **2**, 191 (1951).